Molecular Biology of the Cell
Vol. 18, 2346–2355, June 2007

Induction of Vascular Permeability: βPIX and GIT1 Scaffold the Activation of Extracellular Signal-regulated Kinase by PAK

Rebecca Stockton,*† Jörg Reutershan,* David Scott,* John Sanders,* Klaus Ley,*‡§ and Martin Alexander Schwartz*‡||

*Robert M. Berne Cardiovascular Research Center, and Departments of ‡Biomedical Engineering, §Molecular Physiology and Biological Physics, and ||Microbiology, University of Virginia, Charlottesville, VA 22908

Submitted July 5, 2006; Revised March 26, 2007; Accepted March 30, 2007
Monitoring Editor: Anne Ridley

Increased permeability of blood vessels is an important component of inflammation, but in some circumstances it contributes to tissue injury and organ failure. Previous work showed that p21-activated kinase (PAK) is a critical regulator of endothelial cell–cell junctions through effects on myosin light chain phosphorylation and cell contractility. We now show that blocking PAK function inhibits fluid leak in a mouse model of acute lung injury. In cultured endothelial cells, induction of myosin light chain phosphorylation by PAK is mediated by mitogen-activated protein kinase kinase and extracellular signal-regulated kinase (Erk). Erk in lipopolysaccharide (LPS)-treated mouse lung is activated in a PAK-dependent manner in several cell types, most prominently vascular endothelium. Activation of Erk requires the integrity of the complex between PAK, PIX, and GIT1. Several means of disrupting this complex inhibit stimulation of vascular permeability in vitro. A cell-permeant peptide that blocks binding of PAK to PIX inhibits LPS-induced fluid leak in the mouse lung injury model. We conclude that the PAK–PIX–GIT1 complex is critical for Erk-dependent myosin phosphorylation and vascular permeability.

INTRODUCTION

Vascular permeability is highly regulated in a tissue-specific manner to allow nutrient transport and immune surveillance without excessive leakage of plasma into the tissues (Stevens *et al*., 2000). During inflammation, vascular permeability increases to allow plasma constituents such as antibodies and complement to access injured or infected tissues. However, there are many instances where excessive vascular permeability makes a significant contribution to morbidity and mortality. In myocardial infarction and stroke, vascular permeability induced by vascular endothelial growth factor (VEGF) secretion from ischemic tissue expands the area of tissue damage by severalfold (Stevens *et al*., 2000; Paul *et al*., 2001). In brain injury and infection, vascular permeability is a major contributing factor in coma and death (Kimura *et al*., 2005). In lung injury caused by infection or ventilator-induced overinflation, accumulation of fluid within the alveolae reduces oxygen transport and is a major cause of death (Orfanos *et al*., 2004; Lionetti *et al*., 2005).

We previously reported that PAK phosphorylated on S141 localized to endothelial cell–cell junctions (Stockton *et al*., 2004). PAK 1, -2, and -3 ser/thr kinases are direct effectors for Rac and Cdc42, and they can also be activated by sphingolipids, PDK1, and other mediators (Bokoch, 2003). Activation involves phosphorylation of thr423 (PAK1 numbering), which releases inhibition by the activation loop within the kinase domain, and phosphorylation of ser141, which releases inhibition by the N-terminal inhibitory domain. PAKs are highly multifunctional enzymes for which more than a dozen targets have been identified, including nuclear proteins that control growth and survival, microtubule and actin regulatory proteins, intermediate filament proteins and myosin or myosin-regulatory proteins (Bokoch, 2003). Activation of PAK and localization to cell–cell junctions mediated an increase in myosin light chain (MLC) phosphorylation and disruption of cell–cell junctions (Stockton *et al*., 2004). Remarkably, PAK mediated effects of VEGF, basic fibroblast growth factor (bFGF), histamine, thrombin, and tumor necrosis factor-α on myosin and vascular permeability. Although active PAK inhibits MLC phosphorylation in Chinese hamster ovary cells (Sanders *et al*., 1999), it activates MLC and increases contractility in endothelial cells (Kiosses *et al*., 1999; Zeng *et al*., 2000; Stockton *et al*., 2004). Thus, PAK plays a key role in induction of vascular permeability in response to angiogenic, inflammatory, and thrombotic mediators.

PAK could conceivably activate MLC phosphorylation through several mechanisms. Potential pathways include direct phosphorylation of myosin (Chew *et al*., 1998) or caldesmon (Foster *et al*., 2000). Alternatively, this effect could involve phosphorylation of Raf or mitogen-activated protein kinase kinase (MEK)1/2 to activate extracellular signal-regulated kinase (Erk) (Frost *et al*., 1997; King *et al*., 1998), which can activate myosin light chain kinase (MLCK) (Klemke *et al*., 1997). In this study, we sought to elucidate the mechanism by which PAK activates MLC phosphorylation to in-

This article was published online ahead of print in *MBC in Press* (http://www.molbiolcell.org/cgi/doi/10.1091/mbc.E06–07–0584) on April 11, 2007.

† Present address: Department of Medicine, University of California, San Diego, La Jolla, CA 92093-0623.

Address correspondence to: Martin Alexander Schwartz (maschwartz@virginia.edu).

duce vascular leak and to determine whether this pathway is relevant to permeability in vivo.

MATERIALS AND METHODS

Cell Culture and Transfection

Bovine aortic endothelial cells (BAECs) were grown in low glucose DMEM with 10% bovine calf serum (Atlanta Biologicals, Atlanta, GA), 100 μg/ml dihydrostreptomycin, and 60 U/ml penicillin (Sigma-Aldrich, St. Louis, MO) as described previously (Stockton *et al*., 2004). Human umbilical vein endothelial cells (HUVECs) were from Dr. Brett Blackman (University of Virginia), grown in endothelial growth medium-2 medium (Cambrex Bio Science Walkersville, Walkersville, MD) supplemented with the manufacturer's "SingleQuot" additions plus 10% fetal bovine serum (Atlanta Biologicals), and they were used at passages 3–10.

For some permeability assays on filters, as indicated in figure legends, confluent BAECs in 0.5% calf serum (CS)-DMEM in 100-mm tissue culture dishes were transfected with 5 μg total of the indicated cDNAs by using Effectene (QIAGEN, Valencia, CA) according to the manufacturer's instructions. After incubation overnight, cells were transferred to DMEM with 10% serum and used at 48 h. For some assays, as indicated in legends, cells were transfected by nucleoporation. Cells from two 15-cm plates at 90% confluence were detached and resuspended in 1.5 ml of nucleofection buffer (phenol red-free M199 containing 10 mM HEPES). For each transfection, 100 μl of cell suspension in 0.2-μl cuvettes received 2.5 μg of DNA. Nucleofection was done using the Nucleofector II M3 program cycle (Amaxa Biosystems, Gaithersburg, MD), after which cells were transferred to 60-mm plates containing 5 ml of growth medium and used at 48 h. For immunofluorescence, dishes contained fibronectin (FN)-coated glass coverslips. PAK peptides were synthesized by the Biomolecular Research Facility at the University of Virginia or EZ Biolabs (Westfield, IN), and they were purified by one round of high-performance liquid chromatography.

The βPIX and GIT1 constructs were obtained from Dr. A. F. Horwitz (University of Virginia). The ΔGBD βPIX (mutated for GIT1 binding) and ΔSHD mutant of GIT1 (mutated for PIX and MEK binding) were as described previously (Zhang *et al*., 2003). Dominant-negative MEK1 was as described previously (Renshaw *et al*., 1997). GIT1 Smartpool small interfering RNA (siRNA) oligonucleotides against human sequence were obtained from Dharmacon RNA Technologies (Lafayette, CO), and the experiments were carried out in HUVECs.

Lipopolysaccharide (LPS)-induced Pulmonary Microvascular Permeability

All animal experiments were approved by the Animal Care and Use Committee of the University of Virginia. Wild-type male mice (C57Bl/6, 8–12 wk of age, The Jackson Laboratory, Bar Harbor, ME) were exposed to aerosolized LPS (*Salmonella enteritidis*, Sigma-Aldrich) for 30 min. This results in a significant increase in microvascular permeability (Reutershan *et al*., 2005). Control animals inhaled saline. Some mice received intraperitoneal (i.p.) injection of the PAK inhibitory or control peptides 30 min before LPS exposure. To test the role of MEK in vivo, 0.5 ml of 70 μM UO126 was injected i.p. Permeability was analyzed at 6 h by using the Evans blue dye extravasation technique (Green *et al*., 1988). Evans blue (20 mg/kg; Sigma-Aldrich) was injected intravenously 30 min before euthanasia. Lungs were perfused through the spontaneously beating right ventricle to remove intravascular dye. Lungs were removed, and Evans blue was extracted as described previously (Peng *et al*., 2004). The absorption of Evans blue was measured at 620 nm and corrected for the presence of heme pigments: A_{620} (corrected) = $A_{620} - (1.426 \times A_{740} + 0.030)$ (Wang le *et al*., 2002). Extravasated Evans blue was calculated against a standard curve (micrograms of Evans blue dye per gram of lung).

Immunoprecipitation and Western Blotting

Cells were stimulated, washed with cold phosphate-buffered saline (PBS), extracted with 0.5 ml of cold immunoprecipitation (IP) buffer (20 mM Tris, pH 7.6, 0.5% NP-40, 250 mM NaCl, 5 mM EDTA, 3 mM EGTA; plus Sigma protease and phosphatase inhibitor cocktails) for 10 min. They were passed through an 18-gauge needle three times and centrifuged for 10 min at 12,000 × *g* in a microfuge. Supernatants were precleared with 25 μl of Protein G-agarose beads and incubated with the indicated primary antibody for 2 h at 4°C. Anti-phospho-PAK was from Biosource International (Camarillo, CA); anti-total PAK was from BD Biosciences Transduction Laboratories (Lexington, KY); anti-phospho-Erk and total Erk were from Cell Signaling Technology (Danvers, MA). Anti-GIT1 and anti-βPIX were from Santa Cruz Biotechnology (Santa Cruz, CA). Twenty-five microliters of protein A- or protein G-agarose beads were added and incubated for another 2 h while rotating at 4°C. Beads were sedimented and washed three times with 0.5 ml of IP buffer and separated by SDS-polyacrylamide gel electrophoresis. For binding to peptides, 25 μg of biotin-tagged peptides were incubated with 25 μl of streptavidin beads for 30 min and then rinsed and incubated with 0.5 cell lysates for 30 min. Bound proteins were detected by Western blotting with the indicated antibodies. For βPIX, cells were transfected with hemagglutinin (HA)-PIX, and blots were probed using anti-HA. Proteins were electrophoretically transferred to polyvinylidene difluoride membranes, blocked with 5% milk in Tris-buffered saline, and probed overnight with primary antibodies in the same buffer. Membranes were washed four times, probed with secondary antibodies for 2 h, and then visualized using chemiluminescence (GE Healthcare, Little Chalfont, Buckinghamshire, United Kingdom).

In Vitro Permeability

BAECs on FN-coated 3-μm filters at near-confluence were transfected with 0.5 μg cDNA by using Effectene as described above. At 48 h, cells were pretreated for 60 min with PAK peptides as indicated. For some experiments, cells were nucleofected, and then they were plated on filters and grown to confluence for 48 h. Filters were then placed in outer wells with 500 μl of fresh DMEM without phenol red or serum. To each filter well was added 200 μl of medium plus 50 μl of 1.5 μg/ml horseradish peroxidase (HRP) with or without cytokines as described. After 30 min, filters were removed and fixed, and the medium in the lower wells was assayed for HRP as described previously (Stockton *et al*., 2004). Values were normalized to control, untreated wells.

Immunofluorescence

Cells were fixed for 60 min in 3.5% formaldehyde, washed, and permeabilized for 10 min in 0.2% Triton X-100. Coverslips were blocked with PBS containing 10% goat serum for 60 min, and then they were probed 8 h at 4°C with 200 μl containing the following antibodies: phospho-Erk at 1:500, phospho-MEK at 1:500, phospho-PAK at 1:500, phospho-MLC at 1:500 (all from BioSource International), and βPIX at 1:200 or GIT1 at 1:200 (Santa Cruz Biotechnology). Coverslips were washed and probed overnight at 4°C with 200 μl of anti-mouse immunoglobulin G (IgG)-Alexa 568 or anti-rabbit IgG-Alexa 488 (Invitrogen, Carlsbad, CA) at 1:1000, or Alexa 568-phalloidin at 1:500. Coverslips were washed and mounted using FluoroMount (Invitrogen). Cells were visualized with an MRC 1024 confocal microscope (Bio-Rad, Hercules, CA) mounted on a Nikon Diaphot microscope, with a 60× objective lens (numerical aperture, 1.4) with a pinhole aperture setting of 6. Within an experiment, all cells were treated with the same concentration of Alexa 568-phalloidin, and all images were acquired using same settings.

Image Quantification

For determining the ratio of stress fiber to total actin in images from Figure 7, average pixel intensities were obtained from 25 individual outlined cells per treatment by using Scion Image software (Scion, Frederick, MD). A sharpening filter was applied equally to the images, and then images were thresh-

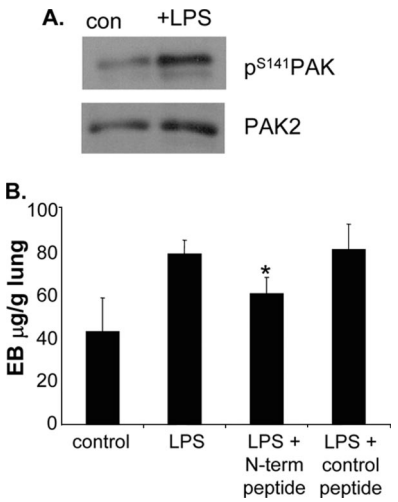

Figure 1. Role of PAK in vascular permeability in a mouse model of lung inflammation. (A) Mice inhaled aerosolized LPS for 30 min, with or without prior intraperitoneal injection of 1 mg of PAK N-terminal peptide or mutated, control peptide. Control animals inhaled saline. At 6 h, lungs were removed, extracted, and analyzed by Western blotting for pSer141 and total PAK2. Two experiments gave similar results. (B) Mice were injected with control or PAK N-terminal peptide and exposed to LPS or saline as described in A. At 6 h, microvascular permeability was determined leakage of Evans blue dye (EB) as described in *Materials and Methods*. Values are means ± SD, n = at least 4. *$p < 0.01$, relative to LPS-treated mice without peptides.

olded and converted to binary masks. The masks were aligned against the original outlined image without altering pixel values. Total cell fluorescence ($pixels_{Mask1}$) and stress fiber fluorescence from the interior of the cell ($pixels_{Mask2}$) were calculated. Values are means ± SE.

For Western blots, NIH ImageJ (http://rsb.info.nih.gov/ij/) was used to evaluate pixel densities. The blots shown are representative of two or three experiments. Signals from indicated phospho-antibody probes were normalized as a percentage of control, total antibody signal from the same blot. Graphs indicate normalized pixel density for the blot shown.

Immunohistochemistry

Mouse lungs were inflated with an intratracheal instillation of 4% paraformaldehyde (PFA) at a constant pressure (20 cm H_2O) for 15 min. Next, lungs were removed and fixed in 4% PFA for 24 h and embedded in paraffin. Sections (5 μm) were cut for immunohistochemistry and treated with antigen unmasking solution (Vector Laboratories, Burlingame, CA). Sections were stained with monoclonal rabbit anti-phospho-Erk (1:400; Cell Signaling Technology) overnight and detected with Vectastain Elite kit (Vector Laboratories). Visualization was done with diaminobenzidine (Dako North America, Carpinteria, CA) and couterstained with hematoxylin. Images were acquired using 20 or 40× objective on a microscope (model BX51; Olympus, Tokyo, Japan) equipped with a digital camera (model DP70; Olympus) by using Image-Pro software program (Media Cybernetics, Silver Spring, MD) in the Academic Computing Health Sciences Center at the University of Virginia.

RESULTS

Inhibiting PAK Decreases Fluid Transport in Acute Lung Injury in Mice

Previous work implicated PAK in regulation of endothelial junctional integrity in vitro (Zeng *et al*., 2000; Stockton *et al*., 2004), but the relevance to vascular permeability in vivo was not determined. To test whether inhibition of PAK decreases vascular leak in vivo, we used a mouse model of acute lung injury in which inhalation of aerosolized LPS triggers fluid accumulation in the lungs (Reutershan *et al*., 2005). Western blotting using an antibody against a phosphorylation site on PAK that is associated with increased PAK kinase activity showed an increase in PAK phosphorylation in lungs from mice exposed to LPS (Figure 1A). The normalized increase was 2.1 ± 0.5-fold relative to control, demonstrating PAK activation in this system.

We previously found that the inhibitory effect of a full-length dominant-negative PAK mapped to the N-terminal proline-rich sequence that binds the Src homology (SH3) domain of Nck (Kiosses *et al*., 1999). A peptide in which this sequence was linked to the polybasic sequence from the human immunodeficiency virus (HIV) TAT protein readily enters cells and blocks PAK function similarly to overexpressed dominant-negative PAK (Kiosses *et al*., 2001). We therefore injected mice with this peptide and examined the leakage of Evans blue dye into the lung after inhalation of LPS. This peptide significantly inhibited dye extravasation, whereas a control peptide in which two prolines essential for SH3 binding were replaced with alanines had no effect (Figure 1B). Although we cannot exclude that this peptide binds other SH3 domain-containing proteins or affects Nck

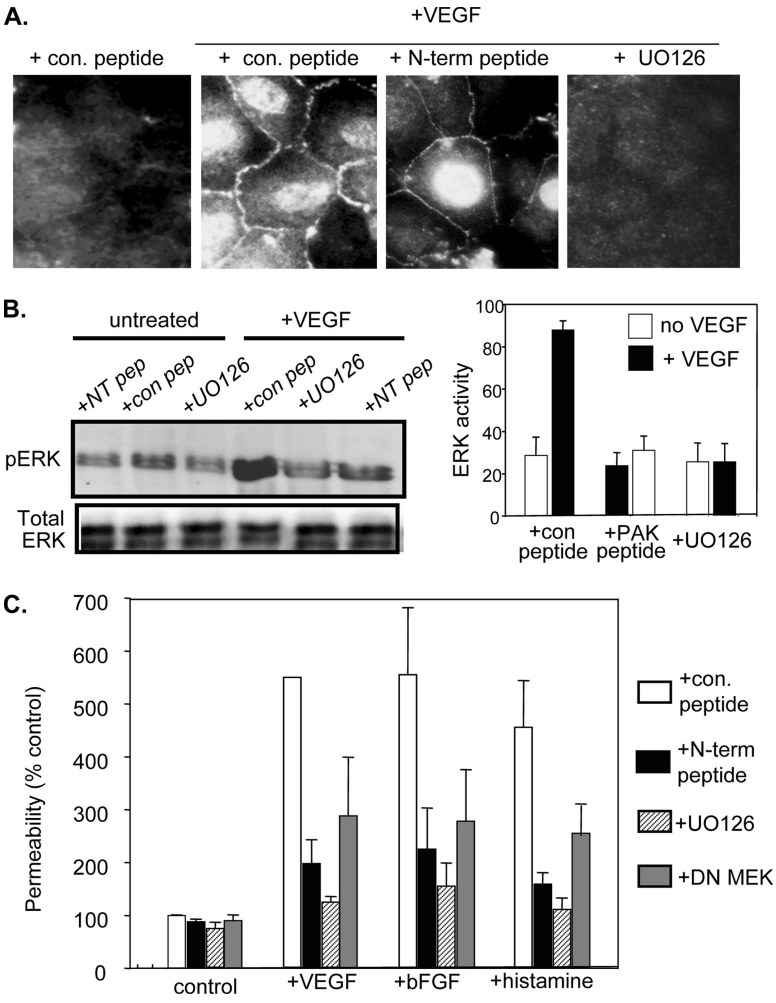

Figure 2. Erk mediates effects on permeability downstream of PAK. (A) BAECs were pretreated with 20 μg/ml PAK N-terminal (NT) peptide that blocks Nck binding; a mutated, control peptide; or the MEK inhibitor U0126 (25 μM). After 1 h, 25 ng/ml VEGF was added for 30 min. Cells were then fixed and stained for activated Erk. (B) Cells as described in A were extracted and analyzed for Erk phosphorylation by Western blotting. Quantitation: values are means ± SE for phospho-Erk normalized total Erk (n = 3). The increase after VEGF in the control sample is statistically significant, as are the differences between VEGF-induced permeability in control versus PAK peptide, and between control and UO126 ($p < 0.01$ in all cases). (C) BAECs on 3-μm filters were transfected with dominant-negative MEK1 (DN MEK), pretreated for 1 h with 20 μg/ml PAK N-terminal peptide or mutated, control peptide, or pretreated with 25 μM U0126. Cells were left untreated or stimulated for 1 h with 25 ng/ml VEGF, 50 ng/ml bFGF, or 10 μM histamine. Leakage of HRP across the filter was assayed as described in *Materials and Methods*. Values are means ± SD, n = 3.

targets other than PAK, the data suggest a role for PAK in regulating permeability in vivo.

A Role for Erk in Vascular Permeability In Vitro

We next considered whether the Erk pathway might be involved. As a first assay, we examined the localization and activation of Erk. Confluent BAECs were used in these experiments as these cells are readily transfectable, and previous work showed that HUVECs and BAECs behaved similarly with respect to PAK and junctional integrity (Stockton *et al*., 2004). Stimulation with VEGF induced an increase in total staining for activated Erk, with a substantial fraction localized to cell–cell borders (Figure 2A). This staining was nearly eliminated by pretreatment with the MEK inhibitor UO126, demonstrating that the signal is specific. The PAK N-terminal peptide was then used to test whether Erk functions downstream of PAK in this pathway. Both immunostaining of monolayers and Western blotting of total cell lysates showed that activation of Erk by VEGF was blocked by the active PAK inhibitory peptide but not the control peptide nearly as well as by the MEK inhibitor UO126 (Figure 2, A and B). Similar results were obtained with bFGF (data not shown).

To investigate effects on vascular permeability in vitro, BAECs were grown on filters with 3-μm pores, and transport of HRP across the monolayer was assayed. Permeability induced by VEGF, bFGF, or histamine was blocked by UO126 or by transfection with dominant-negative MEK as well as by the PAK N-terminal peptide (Figure 2C).

In the mouse model, LPS seems to act by triggering release of cytokines from resident macrophages rather than directly upon the endothelium and epithelium (Maus *et al*., 2002). However, in vitro LPS can increase endothelial permeability directly (Bannerman and Goldblum, 1999); thus, we investigated the role of PAK in this pathway. We also examined responses of endothelial cells to epidermal growth factor (EGF), because this factor was reported to activate Erk via a PAK-independent pathway (Beeser *et al*., 2005). Addition of LPS to endothelial monolayers did not detectably increase phosphorylation of PAK or Erk (Figure 3A). LPS did trigger a reproducible increase in permeability across the monolayer, but it was insensitive to an inhibitory PAK peptide (the PIX-blocking peptide that is discussed below; Figure 3C). EGF increased activation of Erk without a detectable change in PAK phosphorylation (Figure 3A). Activation of Erk and induction of permeability by EGF were unaffected by the PAK inhibitory peptide (Figure 3, B and C). These results indicate that LPS induces permeability through a PAK and Erk-independent pathway, whereas EGF does so via a PAK-independent but Erk-dependent mechanism.

We then addressed whether these results with cultured endothelial cells were applicable to the vasculature in vivo. We first stained lung sections with an antibody to phospho-Erk. In lungs from untreated mice, most of the lung showed little signal except for sparsely distributed cells in the alveolar wall (Figure 4A, small arrows). The identity of these cells is unknown, although resident macrophages or dendritic cells seem likely candidates. In LPS-treated mice, there was a marked increase in Erk activation in many cell types, most prominently the vascular endothelium at specific sites along the vessel wall (Figure 4A, large arrowheads). Alveolae also stained positively, although less so than these sites in blood vessels. This staining may represent alveolar capillaries or epithelium. Treatment of mice with the N-terminal PAK peptide largely prevented Erk activation (Figure 4A), indicating that Erk is downstream of PAK. The control peptide had no effect (data not shown). As a control, mice were

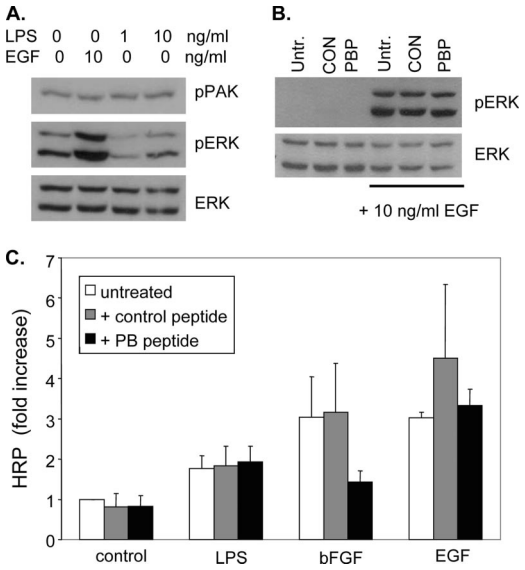

Figure 3. PAK-independent effects of LPS and EGF. (A) BAECs were treated with LPS or EGF at the indicated concentrations for 30 min and then lysed and analyzed by Western blotting for PAK phosphorylation, Erk phosphorylation, and total Erk as a loading control. Similar results were obtained in 3 independent experiments. (B) BAECs were pretreated the inhibitory peptide described in Figure 7 (PIX-blocking peptide; PBP) or inactive control peptide (Con) at 20 μg/ml. They were then stimulated with LPS or EGF. After 30 min, cells were lysed and analyzed by Western blotting for phosphorylated Erk or total Erk. Similar results were obtained in three independent experiments. (C) BAECs on filters were pretreated with PIX-blocking (PB) peptide or control peptide as in Figure 3B and then stimulated with 10 ng/ml LPS, 10 ng/ml EGF, or 25 ng/ml bFGF as indicated. Permeability across the filter was assayed by movement of HRP as described in *Materials and Methods*. Values are means ± SD, n = 3.

pretreated with the MEK inhibitor UO126, which also blocked Erk activation throughout the tissue (Figure 4A). To determine whether Erk is required for vascular leak in this in vivo system, the effect of UO126 was assayed. The MEK inhibitor significantly blocked the induction of permeability by LPS in this model (Figure 4B). We conclude that the MEK–Erk pathway mediates the effect of PAK on vascular permeability.

Involvement of βPIX and GIT1

We next considered the possibility that specific protein interactions may facilitate the activation of Erk downstream of PAK. PAK is known to associate with PIX proteins through binding of an unconventional proline-rich sequence in PAK to the SH3 domain of PIX (Manser *et al*., 1998). PIX also contains a central DH/PH module that has nucleotide exchange activity for Rac and Cdc42, and a region near the C terminus that binds GIT1 (Bagrodia *et al*., 1999; Zhao *et al*., 2000). GIT1 contains an Arf GAP domain and a Spa2-homology domain (SHD) that binds both PIX (Turner *et al*., 2001) and MEK1 and -2 (Premont *et al*., 2004; Yin *et al*., 2004). Thus, the PIX-GIT complex has the potential to bring PAK and MEK into proximity, which might facilitate activation of MEK.

Staining BAEC monolayers with antibodies to βPIX and GIT1 showed that a portion of these proteins were present at cell–cell borders (Figure 5A). Staining of mouse lung sections also showed expression of both βPIX and GIT1 in the

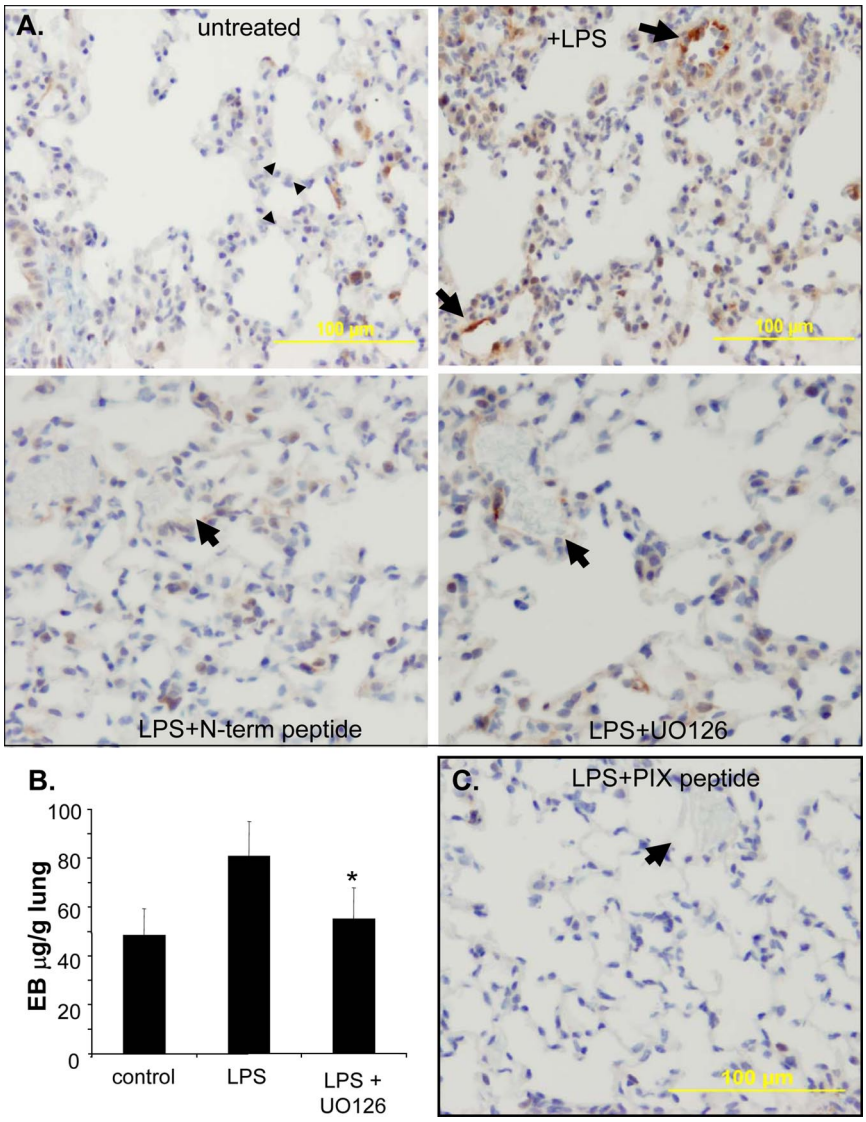

Figure 4. Erk activation in mice after LPS inhalation. (A) Mice were injected intraperitoneally with 1 mg of PAK N-terminal peptide, 1 mg of control peptide, or 0.5 ml of UO126 at 70 μM, and then they were treated with saline or LPS as described in Figure 1. At 6 h, the lungs were removed, fixed, and embedded. They then were sectioned and stained for activated Erk by using pT202/pY204 antibody. Small arrows indicate unidentified cells in control lungs that stain positively. Large arrows indicate conduit blood vessels. (B) Mice were treated with saline or LPS, with or without prior injection of 0.5 ml of MEK inhibitor U0126 at 70 μM. At 6 h, leakage of Evans blue dye (EB) was assayed as described in A. Asterisk (*) indicates statistical significance, $p < 0.05$ relative to LPS-treated mice without UO126; $n \geq 4$. (C) Some mice from the same experiment, described in A were injected with 1 mg/ml PIX blocking peptide, exposed to LPS and sections stained for phospho-Erk. Arrow indicates a conduit vessel.

endothelium (data not shown). Additionally, IPs of phospho-PAK contained active MEK (Figure 5B), consistent with formation of a protein complex. To test the requirement for PIX and GIT1 in these interactions, BAECs were transfected with vectors for wild-type (WT) βPIX or a mutant in which the C-terminal GIT binding domain (GBD) was deleted. When PIX was immunoprecipitated, the ΔGBD PIX reduced the coIP with active MEK (Figure 5C). WT PIX, by contrast, increased MEK coIP.

To investigate the functional relevance of these protein interactions, cells were transfected with WT versus mutant PIX, or with WT GIT1 versus a mutant in which the SHD that binds PIX and MEK was deleted. Cells were stimulated and stained for active PAK. Expression of mutant βPIX or GIT1 completely blocked localization of phospho-S141 PAK to cell–cell junctions, whereas the WT constructs had no effect (Figure 5D). The mutant constructs also blocked activation of Erk and MLC, whereas the WT constructs either increased activation or had no effect (Figure 5, E and F). Finally, both mutant βPIX and GIT1 efficiently blocked the increase in permeability across an endothelial monolayer in vitro in response to VEGF (Figure 6A) and bFGF (data not shown). By contrast, expression of WT constructs modestly increased permeability. We conclude that the PIX–GIT complex plays a critical role in facilitating Erk and MLC activation downstream of PAK.

These results seem to conflict with those from Berk and colleagues who reported that knockdown of GIT1 in HUVECs increased vascular permeability in response to thrombin (van Nieuw Amerongen *et al.*, 2004). To address this discrepancy, we examined the effect of GIT1 knockdown on in vitro permeability in response to multiple soluble factors. We also used HUVECs in these experiments to allow a direct comparison with the previous study and because the sequence for bovine GIT is not available. We found that siRNA oligonucleotides targeting GIT1 decreased protein expression, lowered baseline permeability, and efficiently blocked the increase in permeability induced by bFGF and histamine; however, there was no statistically significant effect on thrombin-induced permeability (Figure 6B). Although we did not see the previously observed enhancement of permeability (van Nieuw Amerongen *et al.*, 2004), it is clear that GIT1 plays a distinct role in the thrombin pathway compared with cytokines. The absence of enhancement may be due to differences in experimental conditions or to different sources of cells.

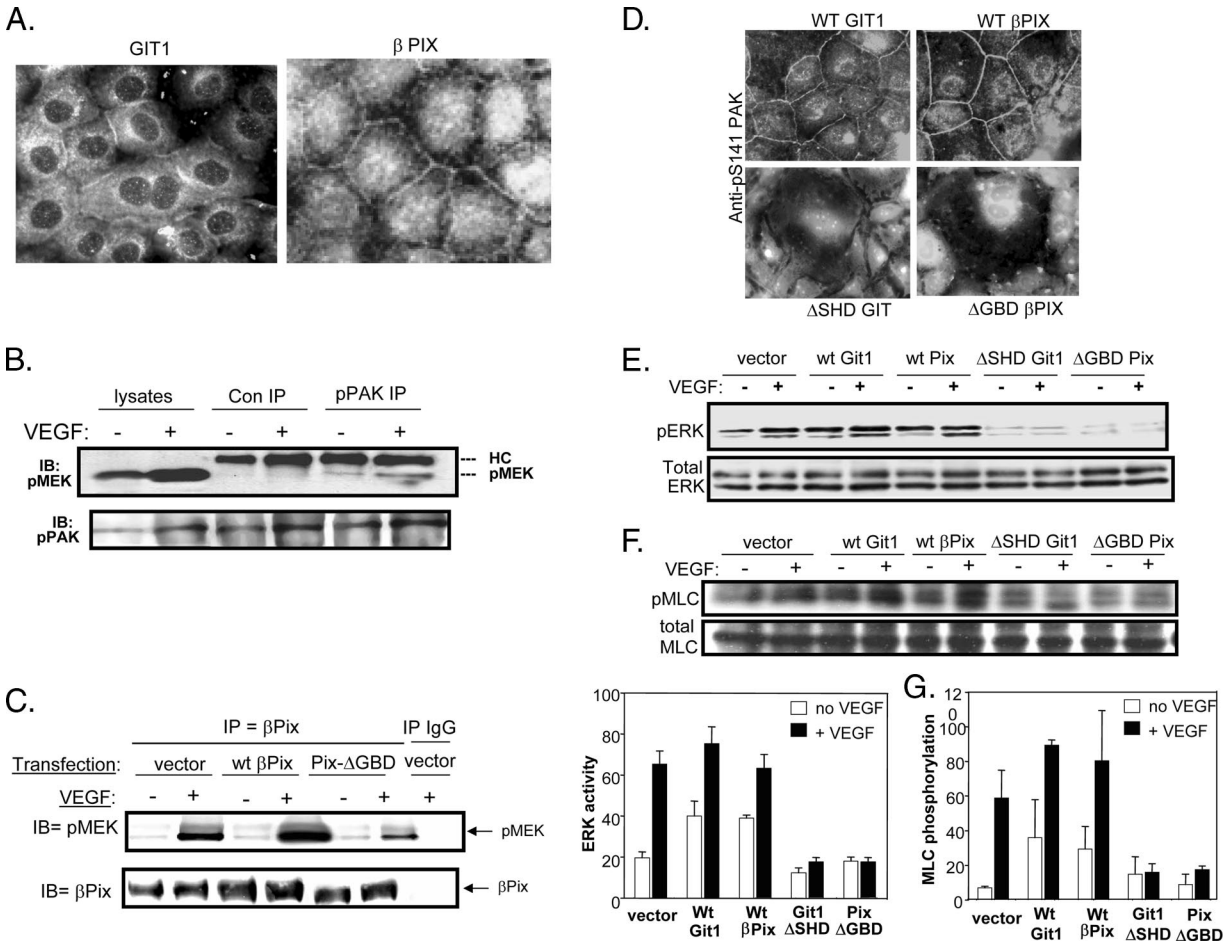

Figure 5. Requirements for βPIX and GIT1 in PAK-dependent permeability. (A) BAECs stimulated with 25 ng/ml VEGF for 30 min were fixed and immunostained for GIT1 or βPIX. (B) BAECs were left untreated or stimulated with VEGF and then extracted and immunoprecipitated with anti-phospho-S141 PAK antibody. The IPs were probes for phospho-MEK1/2, or, as a loading control, for phospho-PAK (pPAK). HC, IgG heavy chain. (C) BAECs were transfected by nucleoporation, using a protocol that gives 80–90% transfection efficiency, with WT PIX or ΔGBD PIX. Starved cells were untreated or stimulated with VEGF as described in A, extracted, and PIX immunoprecipitated. The presence of PIX and active MEK in the IPs was determined by Western blotting. (D) BAECs were nucleoporated with WT GIT1, GIT1 with a SPA2 homology domain (SHD) deletion that does not bind βPIX, WT βPIX, or ΔGBD βPIX. Cells were stimulated with VEGF as described in A and then fixed and stained for phospho-S141 PAK. (E and F) Cells were transfected and stimulated with VEGF as in A, then detergent extracted and analyzed by Western blotting to detect Erk phosphorylation (E) and MLC ser19 phosphorylation (F). (G) Quantitation. For Erk phosphorylation in E, values are means ± SE, n = 3, normalized for total proteins levels. Stimulation by VEGF was statistically significant ($p < 0.01$) as was the decrease in Erk activity after VEGF for GIT1 ΔSHD ($p < 0.01$) and PIX ΔGBD ($p < 0.03$) compared with vector control. For MLC, values are means ± range, n = 2, normalized to total protein levels. Stimulation by VEGF was statistically significant ($p < 0.025$) as was the decrease in Erk activity after VEGF for GIT1 ΔSHD and PIX ΔGBD compared with vector control ($p < 0.04$ for both).

Peptide Inhibition of the PIX–GIT Complex

To further test the functional relevance of the PAK–PIX-GIT complex, we used a peptide inhibitor of PAK–PIX association (Figure 7A). PAK binds to the PIX SH3 domain through an atypical proline-rich region that does not fit the consensus sequences for SH3 binding (Manser *et al.*, 1998). To facilitate its entry into cells, we synthesized a peptide in which this sequence was fused to the HIV TAT polybasic region at its N terminus (Schwarze *et al.*, 1999). We also added a biotin tag to its C terminus to facilitate detection and immobilization for pull-down assays.

When cell lysates were incubated with peptides bound to streptavidin beads, the PIX-blocking peptide bound βPIX with high efficiency (Figure 7B). No binding of βPIX was observed to a control peptide in which two key residues were mutated. Several other SH3-containing proteins showed no binding, although in some experiments cortactin showed weak but specific binding. When higher amounts of cell lysates were used, weak, specific binding of CD2-associated protein (CD2AP) and weak but nonspecific binding of DOCK180 could also be detected (data not shown). The peptide therefore seems to be selective for PIX, although it has other, lower affinity interactions.

To test its ability to disrupt the interaction between PAK and PIX, BAECs were incubated with 20 μg/ml the PIX blocking peptide or the mutated control peptide fused to the TAT sequence to allow entry into cells. The cells were then rinsed, extracted with detergent and βPIX immunoprecipitated. The peptide had no effect on the amount of PIX but reduced the PAK in the precipitates by ~70% (Figure 7C). This result may underestimate the extent of inhibition, because the peptide was washed out before lysis; thus, some reassociation may have occurred during IP. When Erk activation was assayed, the PIX blocking peptide efficiently

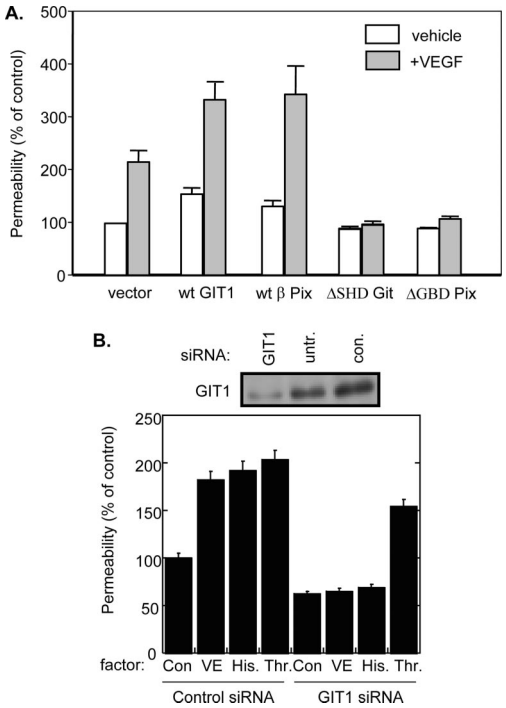

Figure 6. GIT1 and βPIX control permeability in vitro. (A) Cells transfected as in Figure 4C were plated on filters with 3-μm pores at confluent density. Cultures were stimulated with VEGF, and permeability to HRP was assayed as described in *Materials and Methods*. (B) HUVECs were transfected with siRNA oligonucleotides specific to GIT1 or with control, scrambled siRNA. Total cell lysates at 72 h were analyzed for GIT1 expression by Western blotting (top). Cells on filters were analyzed for permeability to HRP after treatment with 50 ng/ml VEGF, 10 μM histamine, or 0.2 U/ml thrombin.

inhibited VEGF stimulation, whereas the control peptide had no effect (Figure 7D). Stimulation of Erk by bFGF was also blocked (data not shown).

We also examined the reorganization of the actin cytoskeleton in response to bFGF (Figure 7E) or VEGF (data not shown). These growth factors triggered an increase in actin stress fibers, which was blocked by the active but not the mutated peptide. These images were quantified to determine the ratio of actin in stress fibers to total actin. In cells treated with control peptide, bFGF increased stress fiber actin from 51 ± 10% to 71 ± 13%, whereas in cells treated with PIX-blocking peptide, basal stress fiber actin was 30 ± 8% and increased to 39 ± 7% after bFGF. These decreases in stress fiber actin induced by the PIX-blocking peptide, both before and after bFGF, are highly significant ($p < 0.0001$). The PIX-blocking peptide at 20 μg/ml also blocked the increase in permeability in vitro in response to VEGF by ~80% in BAECs (Figure 8A) and in HUVECS (data not shown). Similar results were obtained for bFGF (Figure 3C). By contrast, this peptide had no effect on Erk activation and permeability induced by EGF, or permeability induced by LPS, neither of which activate PAK (Figure 3A). The PIX-blocking peptide, therefore, inhibits Erk activation and permeability only for PAK-dependent stimuli. In all cases, the mutant peptide had no effect.

The PIX Blocking Peptide In Vivo

To test whether vascular permeability in vivo requires the interaction between PAK and PIX, we again examined mice

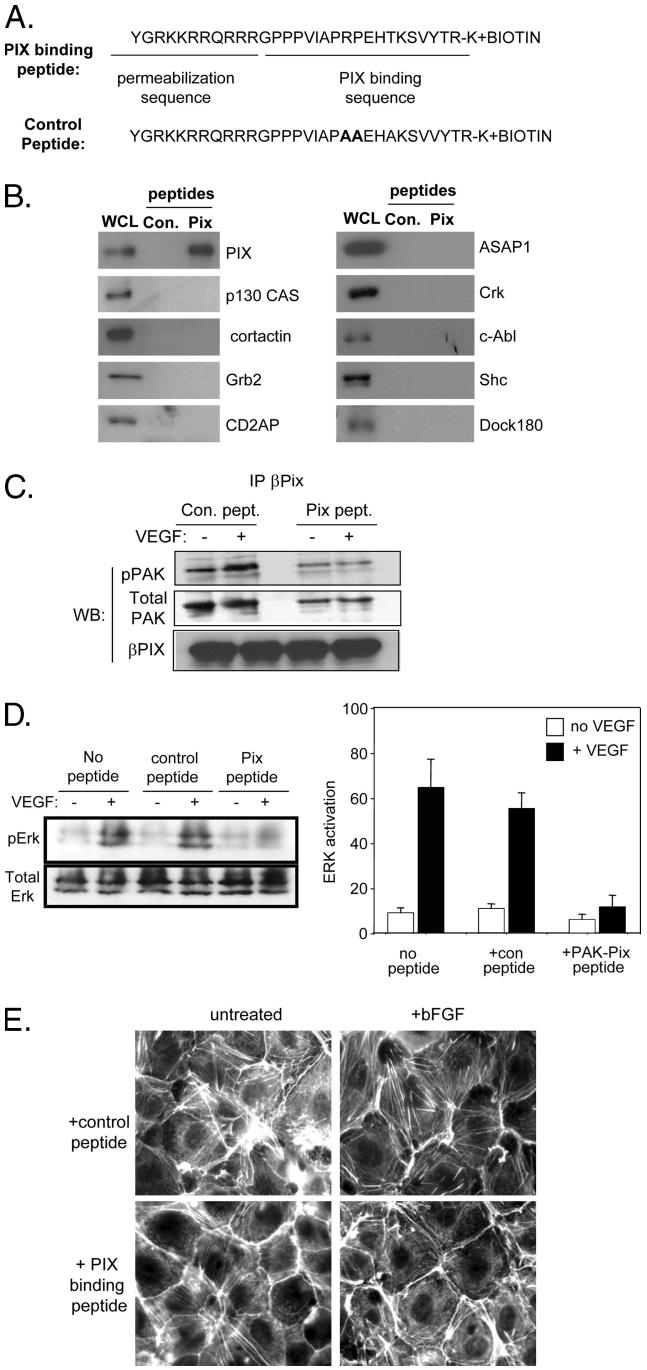

Figure 7. An inhibitory peptide blocks the interaction between PAK and PIX. (A) Sequence of the PIX SH3-blocking peptide and the mutated control. (B) Cell lysates were incubated with PIX-blocking (PIX) or control (Con) peptides immobilized on streptavidin beads. The beads were rinsed, and the bound proteins or whole cell lysates (WCL) or analyzed. Western blots were probed for the indicated SH3 domain-containing proteins. (C) BAECs were incubated with PIX-blocking or control peptide at 20 μg/ml for 1 h and then stimulated with VEGF for 30 min. Cells were rinsed, lysed, and βPIX immunoprecipitated. The IPs were analyzed by Western blotting for PIX as a control, or for PAK and phospho-PAK (pPAK) to detect coIP. (D) BAECs were incubated with peptides and stimulated with VEGF as described in C and then lysed and analyzed for Erk activation by Western blotting against phospho-Erk. Total Erk was analyzed to demonstrate equal loading. Values are means ± SE, n = 3, normalized to total protein. VEGF stimulation of Erk

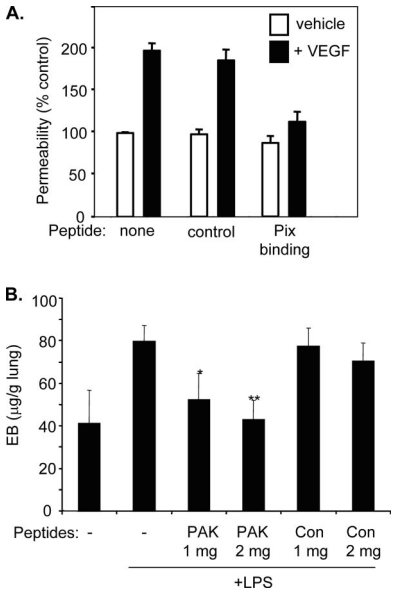

Figure 8. Peptide blocking of the PIX–PAK interaction inhibits permeability. (A) BAECs on filters with 3-μm pores were pretreated with 20 μg/ml PIX-blocking or control peptides for 1 h and then stimulated with VEGF for 30 min. HRP movement across the monolayer was assayed as described in *Materials and Methods*. (B) Mice received intraperitoneal injections with the indicated amounts of the PIX-blocking or control peptides. They were treated with aerosolized LPS or saline for 6 h and then leakage of Evans blue dye (EB) into the lung assayed as described in *Materials and Methods*. Values are means ± SD, n = 4–8. *$p < 0.02$, **$p < .001$, relative to LPS-treated mice without peptides.

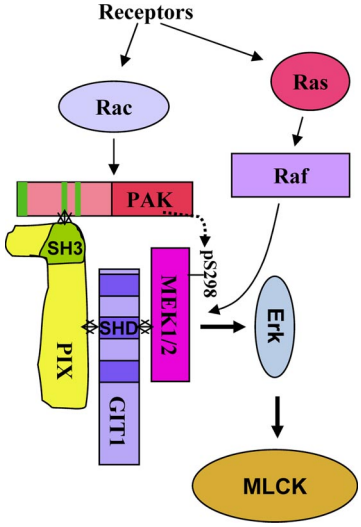

Figure 9. Model for PAK induction of vascular permeability. PAK is activated in response to inflammatory, thrombotic, and angiogenic stimuli. Rac mediates activation of PAK, whereas Ras mediates activation of MEK and Erk. An atypical proline-rich sequence in PAK binds to the βPIX SH3 domain. PIX binds to GIT1 through a region in the C terminus of PIX and the SHD of GIT1. The SHD also binds MEK1/2. PAK phosphorylates MEK on ser298, which facilitates activation of MEK by Raf. Subsequent activation of Erk by MEK leads to activation of MLCK and contractility, which disrupts intercellular junctions.

after inhalation of LPS. For these experiments, we fused the TAT sequence to a version of the PIX blocking peptide that lacked the biotin and the three C-terminal residues, based on an NMR structure showing that these residues did not contribute to the interaction with PIX (Mott *et al*., 2005). Injection of the PIX blocking peptide significantly decreased leakage of Evans blue dye into the lung in a dose-dependent manner (62% inhibition at 1 mg, 85% inhibition at 2 mg), whereas the control peptide had no significant effect (Figure 8B). We also observed inhibition of phospho-Erk staining in lung sections (Figure 4C, arrowhead indicates a blood vessel). We conclude that the complex between PAK and PIX is required for activation of Erk and induction of vascular leak in an in vivo model of lung inflammation.

DISCUSSION

These data show first that PAK is a key regulator of endothelial permeability in a lung injury/inflammation model. Second, PAK seems to act mainly by facilitating Erk activation downstream of multiple cytokines and growth factors. These functional interactions have some selectivity, because LPS can induce permeability in vitro independently of both PAK and Erk, whereas EGF can activate Erk and induce permeability independently of PAK.

Figure 7 (cont). phosphorylation was statistically significant, as was the inhibition byGIT ΔSHD ($p < 0.02$). (E) Cells were incubated with PIX-blocking or control peptides as described in C, stimulated with bFGF for 60 min, and then stained for F-actin.

Multifunctional kinases such as protein kinase A or C that have many potential substrates often use scaffolding and anchoring proteins to enhance specific substrate interactions (Schechtman and Mochly-Rosen, 2001; Scott, 2003). We therefore investigated the role of the PAK–PIX–GIT complex in this pathway. We found that the ability of PAK to activate Erk and induce vascular permeability strongly depends on the integrity of this protein complex. This conclusion is based on colocalization of the relevant components to cell–cell borders, physical association of these components in IPs, and on disruption of the interactions by inhibitory constructs, siRNA-mediated knockdown, and cell-permeant peptides. A model, based on current and published data, is shown in Figure 9. In this model, cytokines trigger activation of PAK through Rac (Stockton *et al*., 2004). PAK is bound to βPIX, where GIT1 binds both PIX and MEK1/2 to bring active PAK into proximity with MEK. PAK then phosphorylates MEK on ser298, which enhances MEK binding and activation by Raf (Frost *et al*., 1997). We speculate that phosphorylated MEK activates Erk, which activates MLCK to promote myosin-dependent contractility as described previously (Klemke *et al*., 1997), leading to disruption of cell–cell junctions (Stockton *et al*., 2004). However, it has also been reported that MEK stimulates vascular permeability independently of Erk (Wu *et al*., 2005). Our data do not address these issues, but these results could be reconciled if a specific subfraction of Erk bound to the appropriate scaffolding proteins mediated these effects. There is precedent for this concept, because the small fraction of Erk that localizes to focal adhesions has properties distinct from total active Erk (Hughes *et al*., 2002). Moreover, recent work showed that PAK also has effects on internalization of VE-cadherin in endothelial cells, which also contributes to permeability (Gavard and Gutkind, 2006).

The requirement for PAK in regulation of permeability is relevant to inflammatory, thrombotic and angiogenic medi-

ators but not for LPS or EGF. The activation of PAK in the LPS inhalation model is likely to be due to a cascade involving several cell types that secrete a variety of factors. Resident lung macrophages are thought to be the primary target for LPS and to secrete cytokines such as macrophage inflammatory protein (MIP)1α and MIP2, which recruits neutrophils and other leukocytes to the tissue (Orfanos *et al*., 2004; Reutershan *et al*., 2005). These cells then secrete additional cytokines. Which of these factors mediate vascular leak has not been addressed in this study. However, the focal nature of Erk activation in the vascular wall suggests that local interactions with leukocytes are likely to be critical. There is evidence that different factors use distinct signaling pathways to induce vascular permeability. VEGF, for example, relies on a src-dependent pathway, whereas bFGF does not (Eliceiri *et al*., 1999). Thrombin effects are mediated mainly by Rho and Rho kinase (Essler *et al*., 1998; van Nieuw Amerongen *et al*., 2004). However, PAK and Erk seem to be common signaling intermediates shared by most of these factors. How these different signaling networks are organized to use the PAK–Erk–MLC axis will be an interesting area for future work.

It is interesting that complete knockdown of GIT1 has effects that are distinct from disruption of the PAK–PIX–GIT complex. Although GIT1 knockdown enhances (van Nieuw Amerongen *et al*., 2004) or has no effect on (our study) thrombin-induced permeability, disruption of the complex blocks in all cases. Thus, it is likely that other activities of GIT1 are involved in modulating the thrombin response. Its Arf GAP activity is an obvious candidate, because it can stimulate focal adhesion disassembly (Turner *et al*., 2001), which is indicative of decreased contractility. Consistent with this idea, suppression of GIT1 expression enhanced focal adhesions in thrombin-treated cells (van Nieuw Amerongen *et al*., 2004). However, specific disruption of PAK–PIX–GIT interactions seem to have distinct effects.

Lung injury is a serious, often fatal, medical problem (Orfanos *et al*., 2004; Lionetti *et al*., 2005). It is commonly caused by infection and can be exacerbated by mechanical ventilation to trigger leakage of fluid into the lungs, leading to respiratory insufficiency. Incidence of death in acute lung injury is in the range of 30–40%, and no specific treatment is currently available. Although the in vivo mouse experiments reported here represent only a first step, the highly encouraging results suggest that further testing is warranted. The PAK peptides or other reagents that block interactions within this protein complex may offer the advantage that other functions of PAK would not be inhibited. Such reagents could conceivably be useful for lung injury or other diseases where vascular permeability is a contributing factor.

ACKNOWLEDGMENTS

We thank Rick Horwitz for the PIX and GIT constructs and James Casanova (University of Virginia) for GIT1 siRNA oligonucleotides. This work was supported by U.S. Public Health Service grants HL-75092 (to M.A.S.) and HL-73361 (to K.L.); a grant from Cryptome Pharmaceuticals (to M.A.S.), and National Institutes of Health Training grant 5T32 HL-7284-27 (to R.S.).

REFERENCES

Bagrodia, S., Bailey, D., Lenard, Z., Hart, M., Guan, J. L., Premont, R. T., Taylor, S. J., and Cerione, R. A. (1999). A tyrosine-phosphorylated protein that binds to an important regulatory region on the cool family of p21-activated kinase-binding proteins. J. Biol. Chem. *274*, 22393–22400.

Bannerman, D. D., and Goldblum, S. E. (1999). Direct effects of endotoxin on the endothelium: barrier function and injury. Lab. Invest. *79*, 1181–1199.

Beeser, A., Jaffer, Z. M., Hofmann, C., and Chernoff, J. (2005). Role of group A p21-activated kinases in activation of extracellular-regulated kinase by growth factors. J. Biol. Chem. *280*, 36609–36615.

Bokoch, G. M. (2003). Biology of the p21-activated kinases. Annu. Rev. Biochem. *72*, 743–781.

Chew, T. L., Masaracchia, R. A., Goeckeler, Z. M., and Wysolmerski, R. B. (1998). Phosphorylation of non-muscle myosin II regulatory light chain by p21-activated kinase (gamma-PAK). J. Muscle Res. Cell Motil. *19*, 839–854.

Eliceiri, B. P., Paul, R., Schwartzberg, P. L., Hood, J. D., Leng, J., and Cheresh, D. A. (1999). Selective requirement for Src kinases during VEGF-induced angiogenesis and vascular permeability. Mol. Cell *4*, 915–924.

Essler, M., Amano, M., Kruse, H. J., Kaibuchi, K., Weber, P. C., and Aepfelbacher, M. (1998). Thrombin inactivates myosin light chain phosphatase via Rho and its target Rho kinase in human endothelial cells. J. Biol. Chem. *273*, 21867–21874.

Foster, D. B., Shen, L. H., Kelly, J., Thibault, P., Van Eyk, J. E., and Mak, A. S. (2000). Phosphorylation of caldesmon by p21-activated kinase. Implications for the Ca(2+) sensitivity of smooth muscle contraction. J. Biol. Chem. *275*, 1959–1965.

Frost, J. A., Steen, H., Shapiro, P., Lewis, T., Ahn, N., Shaw, P. E., and Cobb, M. H. (1997). Cross-cascade activation of ERKs and ternary complex factors by Rho family proteins. EMBO J. *16*, 6426–6438.

Gavard, J., and Gutkind, J. S. (2006). VEGF controls endothelial-cell permeability by promoting the beta-arrestin-dependent endocytosis of VE-cadherin. Nat. Cell Biol. *8*, 1223–1224.

Green, T. P., Johnson, D. E., Marchessault, R. P., and Gatto, C. W. (1988). Transvascular flux and tissue accrual of Evans blue: effects of endotoxin and histamine. J. Lab. Clin. Med. *111*, 173–183.

Hughes, P. E., Oertli, B., Hansen, M., Chou, F. L., Willumsen, B. M., and Ginsberg, M. H. (2002). Suppression of integrin activation by activated Ras or Raf does not correlate with bulk activation of ERK MAP kinase. Mol. Biol. Cell *13*, 2256–2265.

Kimura, R., Nakase, H., Tamaki, R., and Sakaki, T. (2005). Vascular endothelial growth factor antagonist reduces brain edema formation and venous infarction. Stroke *36*, 1259–1263.

King, A. J., Sun, H., Diaz, B., Barnard, D., Miao, W., Bagrodia, S., and Marshall, M. S. (1998). The protein kinase PAK3 positively regulates Raf-1 activity through phosphorylation of serine 338. Nature *396*, 180–183.

Kiosses, W. B., Daniels, R. H., Otey, C., Bokoch, G. M., and Schwartz, M. A. (1999). A role for p21-activated kinase in endothelial cell migration. J. Cell Biol. *147*, 831–843.

Kiosses, W. B., Hood, J., Yang, S., Gerritsen, M. E., Cheresh, D. A., Alderson, N., and Schwartz, M. A. (2001). A dominant negative p65 PAK peptide inhibits angiogenesis. Circ. Res. *90*, 697–702.

Klemke, R. L., Cai, S., Giannini, A. L., Gallagher, P. J., deLanerolle, P., and Cheresh, D. A. (1997). Regulation of cell motility by mitogen-activated protein kinase. J. Cell Biol. *137*, 481–492.

Lionetti, V., Recchia, F. A., and Ranieri, V. M. (2005). Overview of ventilator-induced lung injury mechanisms. Curr. Opin. Crit. Care *11*, 82–86.

Manser, E., Loo, T. H., Koh, C. G., Zhao, Z. S., Chen, X. Q., Tan, L., I. Tan, Leung, T., and Lim, L. (1998). PAK kinases are directly coupled to the PIX family of nucleotide exchange factors. Mol. Cell *1*, 183–192.

Maus, U. A. *et al*. (2002). Role of resident alveolar macrophages in leukocyte traffic into the alveolar air space of intact mice. Am. J. Physiol. *282*, L1245–L1252.

Mott, H. R., Nietlispach, D., Evetts, K. A., and Owen, D. (2005). Structural Analysis of the SH3 domain of beta-PIX and its interaction with alpha-p21 activated kinase (PAK). Biochemistry *44*, 10977–10983.

Orfanos, S. E., Mavrommati, I., Korovesi, I., and Roussos, C. (2004). Pulmonary endothelium in acute lung injury: from basic science to the critically ill. Intensive Care Med. *30*, 1702–1714.

Paul, R., Zhang, Z. G., Eliceiri, B. P., Jiang, Q., Boccia, A. D., Zhang, R. L., Chopp, M., and Cheresh, D. A. (2001). Src deficiency or blockade of Src activity in mice provides cerebral protection following stroke. Nat. Med. *7*, 222–227.

Peng, X., Hassoun, P. M., Sammani, S., McVerry, B. J., Burne, M. J., Rabb, H., Pearse, D., Tuder, R. M., and Garcia, J. G. (2004). Protective effects of sphingosine 1-phosphate in murine endotoxin-induced inflammatory lung injury. Am. J. Respir. Crit. Care Med. *169*, 1245–1251.

Premont, R. T., Perry, S. J., Schmalzigaug, R., Roseman, J. T., Xing, Y., and Claing, A. (2004). The GIT/PIX complex: an oligomeric assembly of GIT

family ARF GTPase-activating proteins and PIX family Rac1/Cdc42 guanine nucleotide exchange factors. Cell Signal *16*, 1001–1011.

Renshaw, M. W., Ren, X. D., and Schwartz, M. A. (1997). Activation of the MAP kinase pathway by growth factors requires integrin-mediated cell adhesion. EMBO J. *16*, 5592–5599.

Reutershan, J., Basit, A., Galkina, E. V., and Ley, K. (2005). Sequential recruitment of neutrophils into lung and bronchoalveolar lavage fluid in LPS-induced acute lung injury. Am. J. Physiol. *289*, L807–L815.

Sanders, L. C., Matsamura, F., Bokoch, G. M., and deLanerolle, P. (1999). Inhibition of myosin light chain kinase by p21-activated kinase. Science *283*, 2083–2085.

Schechtman, D., and Mochly-Rosen, D. (2001). Adaptor proteins in protein kinase C-mediated signal transduction. Oncogene *20*, 6339–6347.

Schwarze, S. R., Ho, A., Vocero-Akbani, A., and Dowdy, S. F. (1999). In vivo protein transduction: delivery of a biologically active protein into the mouse. Science *285*, 1569–1572.

Scott, J. D. (2003). A-kinase-anchoring proteins and cytoskeletal signalling events. Biochem. Soc. Trans. *31*, 87–89.

Stevens, T., Garcia, J. G., Shasby, D. M., Bhattacharya, J., and Malik, A. B. (2000). Mechanisms regulating endothelial cell barrier function. Am. J. Physiol. *279*, L419–L422.

Stockton, R. A., Schaefer, E., and Schwartz, M. A. (2004). PAK regulates endothelial permeability through modulation of contractility. J. Biol. Chem. *279*, 46621–46630.

Turner, C. E., West, K. A., and Brown, M. C. (2001). Paxillin-ARF GAP signaling and the cytoskeleton. Curr. Opin. Cell Biol. *13*, 593–599.

van Nieuw Amerongen, G. P., Natarajan, K., Yin, G., Hoefen, R. J., Osawa, M., Haendeler, J., Ridley, A. J., Fujiwara, K., van Hinsbergh, V. W., and Berk, B. C. (2004). GIT1 mediates thrombin signaling in endothelial cells: role in turnover of RhoA-type focal adhesions. Circ. Res. *94*, 1041–1049.

Wang le, F., Patel, M., Razavi, H. M., Weicker, S., Joseph, M. G., McCormack, D. G., and Mehta, S. (2002). Role of inducible nitric oxide synthase in pulmonary microvascular protein leak in murine sepsis. Am. J. Respir. Crit. Care Med. *165*, 1634–1639.

Wu, M. H., Yuan, S. Y., and Granger, H. J. (2005). The protein kinase MEK1/2 mediate vascular endothelial growth factor- and histamine-induced hyperpermeability in porcine coronary venules. J. Physiol. *563*, 95–104.

Yin, G., Haendeler, H., Yang, C., and Berk, B. C. (2004). GIT1 functions as a scaffold for MEK1-extracellular signal regulated kinase 1 and 2 activation by angiotensin II and epidermal growth factor. Mol. Cell. Biol. *24*, 875–885.

Zeng, Q., Lagunoff, D., Masaracchia, R., Goeckeler, Z., Cote, G., and Wysolmerski, R. (2000). Endothelial cell retraction is induced by PAK2 monophosphorylation of myosin II. J. Cell Sci. *113*, 471–482.

Zhang, H., Webb, D. J., Asmussen, H., and Horwitz, A. F. (2003). Synapse formation is regulated by the signaling adaptor GIT1. J. Cell Biol. *161*, 131–142.

Zhao, Z. S., Manser, E., Loo, T. H., and Lim, L. (2000). Coupling of PAK-interacting exchange factor PIX to GIT1 promotes focal complex disassembly. Mol. Cell. Biol. *20*, 6354–6363.